Top reduced cross section behavior at the LHeC kinematic range

G. R. Boroun[1)]

Physics Department, Razi University, Kermanshah 67149, Iran

Abstract: The linear and non-linear behavior of the top reduced cross section in the LHeC region is considered concerning the boson-gluon fusion (BGF) model for deep inelastic scattering leptoproduction. We show that the non-linear behavior in this region for the $t\bar{t}$ production is very small. The behavior of the top reduced cross section and the ratio R^t in these processes are also considered.

Keywords: Top reduced cross section, nonlinearity, low x behavior

PACS: 13.60.Hb, 12.38.Bx **DOI:** 10.1088/1674-1137/41/1/013104

1 Introduction

Recently there has been important research on $t\bar{t}$ production at the Large Hadron Electron Collider (LHeC) project at CERN [1–3]. The LHeC shows an increase in the kinematic range of the deep inelastic scattering (DIS) and also an increase in the luminosity since this value is approximately $\simeq 100$ fb^{-1}. It would exceed the integrated HERA luminosity by two orders of magnitude. This continues the path of deep inelastic scattering as the best tool to probe proton structure into unknown areas of physics and DIS kinematics. The DIS kinematics are $2 < Q^2 < 100000$ GeV^2 and $0.000002 < x < 0.8$ with a center-of-mass energy of about $\sqrt{s_{\rm ep}} > 1$ TeV in accordance with the B scenario, as the kinematic range of the LHeC is illustrated in Ref. 1. Clearly, there would be an increase in the precision of parton distribution functions (PDFs) and in the low x kinematic region in this project. A strong rise of the reduced cross section is expected to appear due to the non-linear gluon-gluon interaction effects in the so-called saturation region.

In neutral current deep inelastic scattering (NC DIS), the inclusive top electroproduction is dominated by boson-gluon fusion at $x \leqslant 0.1$. Top flavor production has not been explored in NC DIS yet, because the cross section is too small ($\simeq 0.023$ pb).

In the Standard Model, a precise measurement of $t\bar{t}$ production in NC DIS is sensitive to the gluon distribution behavior [2], although an increase of the gluon density towards low x values must be tamed by unitarity reasons (especially at hot spots in the proton).

In the framework of DGLAP dynamics [4–5], considering heavy-flavor physics allowed a great advancement in understanding of heavy quark production dynamics. New measurements of charm and beauty production at LHeC will provide high precision pQCD tests, as the LHeC is the ideal machine for a further extension on top production. As to the measurements of LHeC, events with charm and beauty quarks will increase by nearly 36% and 9% of the total respectively, when compared with HERA data available. Due to the large gluon density at low x, $t\bar{t}$ pair production is dominantly via direct BGF. When heavy flavors are not considered as active, then the most standard pQCD scheme is the fixed flavor number scheme (FFNS). For charm and bottom quarks, at $Q^2 \simeq m^2_{\rm c(b)}$, the FFNS describing $\gamma^* {\rm g} \to {\rm c\bar{c}}({\rm b\bar{b}})$ has $n_{\rm f} = 3(4)$. For $Q^2 \gg m^2_{\rm c(b)}$ variable flavor number schemes (VFNS) with $n_{\rm f}+1$ have been introduced. In this scheme large-log re-summation is performed through QCD evolution of the heavy quark PDFs. For realistic kinematics it has to go to the general mass-VFNS(GM-VFNS), as the x is replaced by $x\left(1+\dfrac{4m^2_{\rm H}}{Q^2}\right)$. Different variants of the GM-VFNS scheme are used in the context of global fits of PDFs of the CETQ and MRST groups based on small x DIS data, as it leads to a significant change in the gluon and heavy quark distributions. Here we consider the top flavor physics in the framework of FFNS [6–7] with $n_{\rm f} = 5$. In general the measurement of the top structure function $F_2^{t\bar{t}}$ is of the highest interest for theoretical analysis of top quarks in the final state. At sufficiently high Q^2 the top structure function can be directly related to effective densities of the top quark in the proton.

Received 3 August 2016, Revised 2 September 2016

1) E-mail: boroun@razi.ac.ir

The main purpose of this paper is the top reduced cross section behavior in the LHeC regions. The top reduced cross section will be presented in Section 2. The nonlinear behavior is derived in Section 3. Section 4 contains the discussion and conclusions.

2 Top reduced cross section

We discuss the heavy flavor structure function $F_2(x,Q^2,m_{\rm H}^2)$, which is sensitive to the shape of the gluon density at low x. The reaction under study is $e(p_e)+P(p)\to e(p'_e)+H(p_1)\overline{H}(p_1)+X$, where $H\overline{H}$ are heavy quark-antiquark pairs, such as $c\overline{c}, b\overline{b}$ or $t\overline{t}$, with momentum p_1 ($p_1{}^2=m_{\rm H}^2$) and X is any hadronic state allowed. These pair productions are dependent on the momentum carried by gluon distribution at low x. In the following, we want to determine the reduced cross section of the top pair production in the LHeC region, although this cross section in NC DIS is small [3]. The top reduced cross section is given by the following form

$$\widetilde{\sigma}^t(x,Q^2,m_{\rm t}^2)=F_2^t(x,Q^2,m_{\rm t}^2)\left[1-\frac{y^2}{1+(1-y)^2}R^t\right], \quad (1)$$

where $R^t=\dfrac{F_L^t}{F_2^t}$. The inclusive top structure functions (F_2^t and F_L^t) at leading order (LO) up to next-to-leading order (NLO) analysis are given in Ref. [8] (where only the gluon distributions are considerable). The top structure functions are given by the following forms

$$F_k^t(x,Q^2,m_{\rm t}^2)\simeq\frac{Q^2\alpha_s}{4\pi^2m_{\rm t}^2}\int_x^{z_{\max}}\frac{{\rm d}z}{z}[e_{\rm t}^2g\left(\frac{x}{z},\mu_{\rm t}^2\right)C_{k,g}^{(0)t}$$
$$+\frac{Q^2\alpha_s^2}{\pi m_{\rm t}^2}\int_x^{z_{\max}}\frac{{\rm d}z}{z}[e_{\rm t}^2g\left(\frac{x}{z},\mu_{\rm t}^2\right)(C_{k,g}^{(1)t}+\overline{C}_{k,g}^{(1)t}\ln\frac{\mu_{\rm t}^2}{m_{\rm t}^2}), \quad (2)$$

where $k=2,L$ and the upper boundary on the integration is given by $z_{\max}=\dfrac{Q^2}{Q^2+4m_{\rm t}^2}$, with $m_{\rm t}=175$ GeV. One can consider the boundary condition according to the LHeC region, such that $z_{\max}\to 0.9$ when $Q^2>4m_{\rm t}^2$, $z_{\max}\to 0.5$ when $Q^2=4m_{\rm t}^2$ and $z_{\max}\to 0$ when $Q^2<4m_{\rm t}^2$. Here $g(x,\mu_{\rm t}^2)$ is the gluon density and the scale $\mu_{\rm t}\left(=\sqrt{\dfrac{Q^2}{2}+4m_{\rm t}^2}\right)$ is the mass factorization and the renormalization scale. The $\overline{\rm MS}$ gluonic coefficient functions, $\{C_{k,g}^{(i)t}(\eta,\xi),\overline{C}_{k,g}^{(i)t}(\eta,\xi),i=0,1\}$, originate from those gluonic subprocesses where the virtual photon is coupled to the top pair quark via boson-gluon fusion and they are dependent on the scaling variables $\eta\to\dfrac{s}{4m_{\rm t}^2}$ and $\xi=\dfrac{Q^2}{m_{\rm t}^2}$. The top reduced cross section has been defined in Ref. [2]. Now, let us introduce the compact formula for the ratio R^t such that

$$R^t=\frac{C_{L,g}^{(i)t}(x,\xi)\otimes g(x,\mu_{\rm t}^2)}{C_{2,g}^{(i)t}(x,\xi)\otimes g(x,\mu_{\rm t}^2)}, \quad (3)$$

where the symbol $\otimes$ indicates convolution over the variable x as: $a\otimes b[x]=\displaystyle\int_x^1\frac{{\rm d}z}{z}a(z)b\left(\frac{x}{z}\right)$. The ratio R^t, in top-quark leptoproduction, is a probe of the top content of the proton which greatly simplifies the extraction of F_2^t from measurements of the top reduced cross sections at the LHeC. Figure 1 shows the quantities R^c, R^b and R^t as a function of Q^2 for $x\leqslant 0.01$. The ratios R^c and R^b have approximately the same behavior and they are different from the ratio R^t as these quantities are dependent on the gluon momentum, such that $x_g^t>x_g^b>x_g^c$ (in accordance with the heavy quark mass). These ratios are approximately independent of x at low x values.

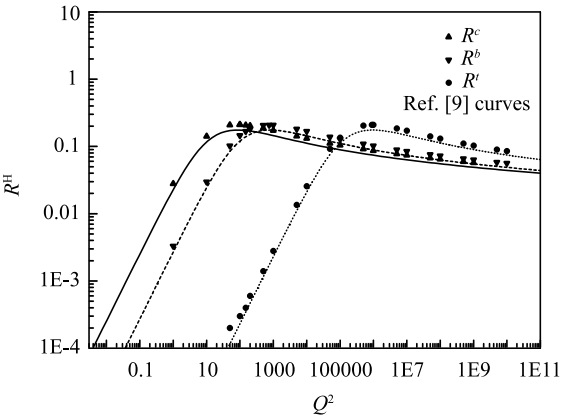

Fig. 1. $R^{\rm H}$ values as functions of Q^2 in NLO analysis with $<\mu_{\rm H}^2>=4m_{\rm H}^2+\dfrac{Q^2}{2}$, compared with curves estimated in Ref. [9].

In Table 1, we see that $R^{\max}\simeq 0.21$ for heavy quarks in a wide region of Q^2. We observe that the $R^{\max}$ predictions occur in the region $Q^2>4m_{\rm H}^2$, as the ratios $\dfrac{Q^2}{4m_{\rm H}^2}$ are 11.11, 8.98 and 8722.46 for production of charm, beauty and top quarks respectively. One can consider the coefficient of R^t on a wide scale of the inelasticity y, such that $\dfrac{y^2}{1+(1-y)^2}\to 1$ at the LHeC region and according to the center of mass energy.

Table 1. Maximum values of $R^{\rm H}$ extracted from Eq. (3).

$Q^2/{\rm GeV}^2$	$R^c_{\max}$	$R^b_{\max}$	$R^t_{\max}$
100	0.2106	—	—
750	—	0.2086	—
860000	—	—	0.2093

Thus the top reduced cross section can be rearranged by

$$\widetilde{\sigma}^t(x,Q^2,m_{\rm t}^2)=F_2^t(x,Q^2,m_{\rm t}^2)[1-R^t]. \tag{4}$$

At $Q^2 \geqslant m_{\rm t}^2$, the top structure function can be evaluated from the top reduced cross section according to Eq. (4) as $F_2^t(x,Q^2,m_{\rm t}^2)=\widetilde{\sigma}^t(x,Q^2,m_{\rm t}^2)/[1-R^t]$ which implies that the R^t values are given by Eq. (3). The gluon distribution of the top structure function is taken from MMHT14 [10], NNPDF3 [11] and CT14 [12] at large scale $\mu_{\rm t}^2$. In what follows we need an analytical form for the gluon distribution. So we shall use the BDHM analysis [13], which is extrapolated to very low x values and high Q^2 values. The results (F_2^t and $\widetilde{\sigma}^t$) of our analysis at $Q^2 \geqslant m_{\rm t}^2$, for top electroproduction, are shown in Fig. 2. It shows that the contribution of the top longitudinal structure function F_L^t to the top reduced cross section will be measurable in the LHeC kinematic range.

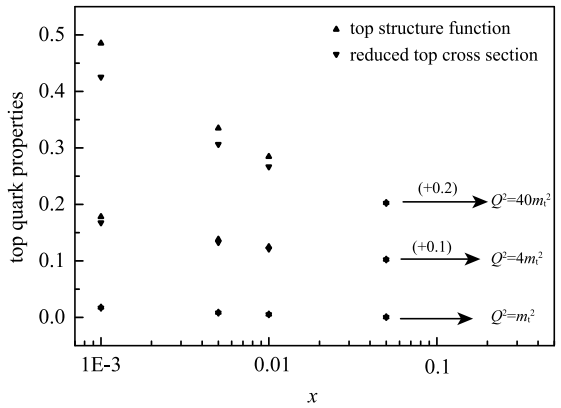

Fig. 2. Top structure function F_2^t and top reduced cross section $\widetilde{\sigma}^t$ determined from Eq. (4) at $Q^2=m_{\rm t}^2, 4m_{\rm t}^2$ and $40m_{\rm t}^2$ GeV^2 for the LHeC region.

For $Q^2 < m_{\rm t}^2$, the ratio R^t is very small. So with a good accuracy we will have

$$\widetilde{\sigma}^t(x,Q^2,m_{\rm t}^2) \simeq F_2^t(x,Q^2,m_{\rm t}^2). \tag{5}$$

At low x, where only the gluon contributions are considerable, the top contribution F_2^t to the proton structure function is given by the form

$$F_2^t(x,Q^2,m_{\rm t}^2)=2e_{\rm t}^2\frac{\alpha_s(\mu_{\rm t}^2)}{2\pi}\int_{1-\frac{1}{a}}^{1-x}{\rm d}zC_{2,g}^{(i)t}\left(1-z,\frac{Q^2}{\mu_{\rm t}^2}\right) \times G\left(\frac{x}{1-z},\mu_{\rm t}^2\right), \tag{6}$$

where $a=1+4\dfrac{m_{\rm t}^2}{Q^2}$, $G=xg$ is the gluon distribution function and $C_{2,g}^{(i)t}$ are the top coefficient functions at LO and NLO analysis. In what follows it is convenient to directly use the gluon distribution behavior according to the Eq. (6) as the top reduced cross section (Eq. (5)) modified by

$$\widetilde{\sigma}^t(x,Q^2,m_{\rm t}^2)\propto C_{2,g}^{(i)t}\left(a_s,x,\frac{Q^2}{\mu_{\rm t}^2}\right)\otimes G(x,\mu_{\rm t}^2). \tag{7}$$

This equation is valid when we apply the high gluon density in accordance with the LHeC region at low x values. It provides a transition from the dilute side by decreasing x or by increasing the number of gluons in the proton. We will study this transition from the linear QCD evolution equations into the non-linear equations in the next section.

3 Nonlinearity

Within the standard framework of leading-twist linear QCD evolution equations (DGLAP), the gluon densities are predicted to rise at low x which was seen in DIS experiments at HERA. At the LHeC low x domains, we expect that the growth of the top reduced cross section, with respect to the gluon densities, saturates by the unitarity bound (caused by Froissart and Martin bounds [14]). This increase at low x should eventually be tamed by the nonlinear effects of gluon density and this occurs when the chance of two gluons recombining into one, i.e. gluon recombination, is higher than gluon splitting. This nonlinear evolution leads to the saturation of gluonic density in the nucleon, which can be exploited for DIS at the LHeC at high centre-of-mass energy(i.e. extending the kinematic range to lower x).

This recombination leads to a modification of the linear DGLAP evolution equation by a term which is nonlinear in gluon density. The first equation of this type reporting the fusion of two gluon ladders into one. This picture allows us to write the Gribov-Levin -Ryskin-Mueller-Qiu (GLR-MQ) [15–16] equation for the gluon distribution at low x. In the double leading logarithmic approximation (DLLA, $\ln 1/x \ln Q^2 >> 1$), GLR-MQ has been determined a new nonlinear evolution equation for gluon density because the negative sign in front of the nonlinear term is responsible for the gluon recombination, as:

$$Q^2\frac{\partial^2 G(x,Q^2)}{\partial \ln\dfrac{1}{x}\partial Q^2}=\frac{\alpha_s N_c}{\pi}G(x,Q^2) -\frac{4\alpha_s^2 N_c}{3C_F R^2}\frac{1}{Q^2}[G(x,Q^2)]^2, \tag{8}$$

in which the parameter R controls the strength of the nonlinearity and it is the correlation radius between two interaction gluons when gluons are concentrated in the hot-spot [17] point ($R \simeq 2$ GeV^{-1}) within the proton.

Thus the Q^2 evaluation of the gluon distribution function (Eq. (8)) with nonlinear effects can be rewritten as

$$\frac{\partial G(x,Q^2)}{\partial \ln Q^2} = \frac{\partial G(x,Q^2)}{\partial \ln Q^2}|_{\rm DGLAP} - \frac{81\alpha_s^2}{16R^2Q^2}\int_\chi^1 \frac{{\rm d}y}{y}[G(y,Q^2)]^2, \quad (9)$$

where $\chi = \dfrac{x}{x_0}$ and $x_0 = 0.01$ is the boundary condition between the shadowing and unshadowing region where the gluon distribution joins smoothly onto the unshadowed region ($x > x_0$). The first term in the r.h.s of Eq. (9) is the standard linear DGLAP evolution that can be expressed at low x as

$$\frac{\partial G(x,Q^2)}{\partial \ln Q^2}|_{\rm DGLAP} \simeq \frac{\alpha_s}{2\pi}[P_{gg}(x,\alpha_s)\otimes G(x,Q^2)], \quad (10)$$

where the splitting function P_{gg} can be ordered in running coupling constant $\alpha_s(Q^2)$. The second term in the r.h.s of Eq. (9) is the nonlinear shadowing term. This shadowing effect arises from the two gluon ladders recombining into a single one. Therefore the gluon distribution function is modified by the following form [18–19]

$$\frac{\partial G(x,Q^2)}{\partial \ln Q^2} = \frac{\alpha_s}{2\pi}P_{gg}(x,\alpha_s)\otimes G(x,Q^2) - \frac{81\alpha_s^2}{16R^2Q^2}\int_\chi^1 \frac{{\rm d}y}{y}[G(y,Q^2)]^2. \quad (11)$$

The solution of Eq. (11) is straightforward and is given by

$$G(x,Q^2) = \frac{M(x,Q^2)}{C - N(x,Q^2)\Gamma[-1+M(x),Q^2]}, \quad (12)$$

in which the functions of M and N are dependent on the coefficients of $G(x,Q^2)$ and $G^2(x,Q^2)$ in the r.h.s of Eq. (11) respectively; Γ is the incomplete gamma function and C is dependent on the initial condition of the gluon distribution at $Q^2 = Q_0^2$. The shadowing correction to the gluon distribution at the initial scale is defined by $G(x,Q_0^2)$. The low x behavior of the shadowing corrections to the gluon distribution at Q_0^2 is assumed to be [20]

$$G(x,Q_0^2) = G^u(x,Q_0^2)[1+\theta(x_0-x)[G^u(x,Q_0^2) - G^u(x_0,Q_0^2)]/G^{\rm sat}(x,Q_0^2)]^{-1}, \quad (13)$$

where $G^{\rm sat}(x,Q^2) = \dfrac{16R^2Q^2}{27\pi\alpha_s(Q^2)}$ is the value of the gluon which would saturate the unitarity limit in the leading shadowing approximation and $G^u(x,Q_0^2)$ is the input unshadowing gluon distribution taken from the QCD parametrisation.

Now, we have the shadowing correction to the initial gluon distribution, so then inserting Eq. (13) in Eq. (12) makes the C constant in Eq. (12) dependent on the initial condition as follows:

$$G(x,Q^2) = \frac{M(x,Q^2)G^u(x,Q_0^2)}{M(x,Q_0^2)\left[1+\dfrac{\theta(x_0-x)[G^u(x,Q_0^2)-G^u(x_0,Q_0^2)]}{G^{\rm sat}(x,Q_0^2)}\right]+\{N(x,Q_0^2)\Gamma[-1+M(x),Q_0^2]-N(x,Q^2)\Gamma[-1+M(x),Q^2]\}G^u(x,Q_0^2)}. \quad (14)$$

Therefore the shadowing correction to the top reduced cross section corresponds to the nonlinear gluon distribution function at scale $\mu_{\rm t}^2$ by the following form:

$$\widetilde{\sigma}^t(x,Q^2,m_{\rm t}^2) \simeq 2e_{\rm t}^2\frac{\alpha_s(\mu_{\rm t}^2)}{2\pi}C_{2,g}^{(i)t}\left(a_s,x,\frac{Q^2}{\mu_{\rm t}^2}\right)\otimes \frac{M(x,\mu_{\rm t}^2)G^u(x,\mu_{0{\rm t}}^2)}{M(x,\mu_{0{\rm t}}^2)\left[1+\dfrac{\theta(x_0-x)[G^u(x,\mu_{0{\rm t}}^2)-G^u(x_0,\mu_{0{\rm t}}^2)]}{G^{\rm sat}(x,\mu_{0{\rm t}}^2)}\right]+\{N(x,\mu_{0{\rm t}}^2)\Gamma[-1+M(x),\mu_{0{\rm t}}^2]-N(x,\mu_{\rm t}^2)\Gamma[-1+M(x),\mu_{\rm t}^2]\}G^u(x,\mu_{0{\rm t}}^2)}. \quad (15)$$

This equation shows that the top reduced cross section behavior is tamed due to the saturation effects at low x. At the LHeC region for $Q^2 < 1000$ GeV^2 we observed that $\mu_{\rm t}^2 \simeq 4m_{\rm t}^2$, therefore the coefficient of the nonlinear term (second term in the r.h.s of Eq. (9)) is very very small and the shadowing correction to the top reduced cross section is not worthwhile. We believe that this behavior for the nonlinear term at low Q^2 values is correct, because within the color dipole approach [21] the $t\bar{t}$ color dipole size is much smaller than the charm and bottom

size ($0.037 \leqslant r_{\rm c} \leqslant 0.130$ fm and $0.014 \leqslant r_{\rm b} \leqslant 0.043$ fm) as

$$\frac{4}{Q^2+4m_{\rm t}^2} \leqslant r_{\rm t}^2 \leqslant \frac{1}{m_{\rm t}^2} \Rightarrow r_{\rm t} \simeq 0.0013 \text{ fm}. \quad (16)$$

We observe that the minimum and maximum distances, related to the $t\bar{t}$ interaction in the color dipole model, are the same value, 0.0013 fm. The color dipole size shows the sticking of the $t\bar{t}$ pair production, therefore in this case the nonlinear effects can be neglected for the LHeC region. So we can conclude that the shadowing corrections to the top reduced cross sections are very small in the LHeC region. On the other hand, in the region of low-x and Q^2 values, the process of gluon recombination does not play an important role in $t\bar{t}$ production and therefore the nonlinear corrections to the top reduced cross section are not essential in this region. In Fig. 3 we show our results for $Q^2 = 100$ GeV^2. The top reduced cross sections are very small for these measurements.

4 Conclusion

We have obtained the ratio $R^t = F_2^t/F_L^t$ at the LHeC regions for top pair production. We demonstrated the relation between the top reduced cross section and the top structure function by this ratio (R^t) at $Q^2 \geqslant m_{\rm t}^2$ and $Q^2 < m_{\rm t}^2$ regions. The linear and nonlinear behaviors were considered and show that the nonlinear behavior has a very low probability at very low x in which gluon saturation is dominant.

Author is grateful to Prof.N.Armesto for suggestion, reading the manuscript and useful comments.

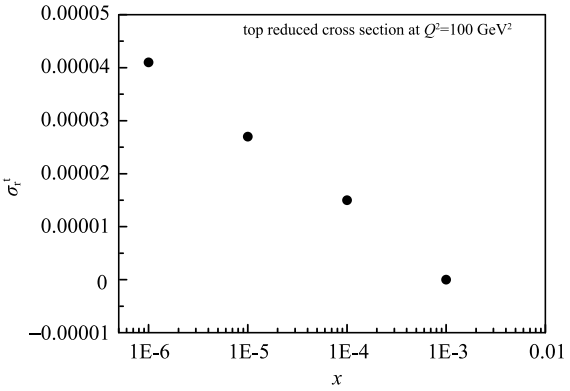

Fig. 3. Top reduced cross section $\widetilde{\sigma}^t$ determined from Eq. (15) at $Q^2 = 100$ GeV^2 for the LHeC region.

References

1 LHeC workshops 2015, (http://cern.ch/lhec)
2 G. R. Boroun, Phys. Lett. B, **744**: 142(2015)
G. R. Boroun, Phys. Lett. B, **741**: 197(2015)
3 J. L. Abelleira Fernandez et al (LHeC Collaboration), J. Phys. G, **39**: 075001(2012)
4 V. N. Gribov and L. N. Lipatov, Sov. J. Nucl. Phys., **18**: 438(1972)
5 L. N. Lipatov, Sov. J. Nucl. Phys., **20**: 93(1975); G. Altarelli and G. Parisi, Nucl. Phys. B, **126**: 298(1977); Yu. L. Dokshitzer, Sov. Phys. JETP, **46**: 641(1977)
6 M. A. G. Aivazis et al, Phys. Rev. D, **50**: 3102(1994)
7 J. C. Collins, Phys. Rev. D, **58**: 094002(1998)
8 E. Laenen, S. Riemersma, J. Smith, and W. L. van Neerven, Nucl. Phys. B, **392**: 162(1993); S. Riemersma, J. Smith, and W. L. van Neerven, Phys. Lett. B, **347**: 143(1995)
9 A. Y. Illarionov, B. A. Kniehl, and A. V. Kotikov, Phys. Lett. B, **663**: 66(2008)
10 L. A Harland-Lang et al, Eur. Phys. J. C, **75**: 435(2014)
11 Richard D. Ball et al (NNPDF Collaboration), JHEP, **04**: 040(2015)
12 S. Dulat et al, arXiv: 1506. 07443
13 M M. Block et al, Phys. Rev. D, **88**: 014006(2013); Phys. Rev. D, **88**: 013003(2013)
14 M. Froissart, Phys. Rev. **123**: 1053(1961); A. Martin, Phys. Rev., **129**: 1432(1963)
15 L. V. Gribov, E. M. Levin, and M. G. Ryskin, Phys. Rep. **100**: 1(1983)
16 A. H. Mueller and J. Qiu, Nucl. Phys. B, **268**: 427(1986)
17 E. M. Levin and M. G. Ryskin, Phys. Rep., **189**: 267(1990)
18 G. R. Boroun, JETP, **106**: 701(2008); G. R. Boroun and B. Rezaei, Eur. Phys. J. C, **73**: 2412(2013)
19 G. R. Boroun, Eur. Phys. J. A, **42**: 251(2009); G. R. Boroun and S. Zarrin, Eur. Phys. J. Plus, **128**: 119(2013)
20 A. D. Martin, W. J. Stirling, R. G. Roberts, and R. S. Thorne, Phys. Rev. D, **47**: 867(1993); J. Kwiecinski, A. D. Martin, and P. J. Sutton, Phys. Rev. D, **44**: 2640(1991); A. J. Askew, J. Kwiecinski, A. D. Martin, and P. J. Sutton, Phys. Rev. D, **47**: 3775(1993)
21 R. Fiore, N. N. Nikolaev, and V. R. Zoller, JETP Lett., **90**: 319(2009)